The Oceanic Vertical Pump Induced by Mesoscale and Submesoscale Turbulence

Patrice Klein[1] and Guillaume Lapeyre[2]

[1]Laboratoire de Physique des Océans, IFREMER, BP 70, Plouzané, France; email: patrice.klein@ifremer.fr

[2]Laboratoire de Météorologie Dynamique/IPSL, Ecole Normale Supérieure/CNRS, 75005 Paris, France; email: glapeyre@lmd.ens.fr

Annu. Rev. Mar. Sci. 2009. 1:351–75

First published online as a Review in Advance on September 10, 2008

The *Annual Review of Marine Science* is online at marine.annualreviews.org

This article's doi: 10.1146/annurev.marine.010908.163704

1941-1405/09/0115-0351$20.00

Key Words

submesoscale structures, biogeochemical tracers, surface frontogenesis, vertical fluxes, turbulent eddy interactions

Abstract

The motivation to study the vertical exchanges of tracers associated with mesoscale eddies is that the mean concentration of most oceanic tracers changes rapidly with depth. Because mesoscale processes may transport these tracers vertically, biogeochemists hypothesized that these vertical exchanges may strongly affect global tracer budgets. This hypothesis has motivated a large number of biogeochemical studies that we review here by focusing on the significant advances that have been achieved and the remaining issues and uncertainties. The main question that emerges concerns the importance of the submesoscales (10 km in the horizontal) in these vertical exchanges. Independently, in the past decade, fluid dynamicists examined the three-dimensional properties of submesoscales generated by a mesoscale (100 km in the horizontal) turbulent eddy field. We review their results and discuss how the vertical exchanges associated with these submesoscales may answer the issues raised by biogeochemical studies and inspire future directions.

INTRODUCTION

The oceanic circulation is characterized not only by large-scale currents such as the Gulf Stream or the Kuroshio, but also by energetic mesoscale structures, the oceanic cyclonic and anticyclonic eddies that are the ocean counterparts of the weather systems. Such eddies are ubiquitous features that can be seen in the altimeter signal (LeTraon & Morrow 2001, Isern-Fontanet et al. 2006b, Chelton et al. 2007) or in infrared and color satellite images (Johannessen et al. 1996). These eddies have a diameter of 50–200 km and their core is located as deep as 2000 m. These eddies involve dynamical anomalies [such as sea surface height (SSH) and density anomalies] with large amplitudes. Infrared and color images have also highlighted the presence of a rich organization of smaller-scale (or submesoscale) structures between the eddies (**Figure 1**). These submesoscale structures are filaments elongated over hundreds of kilometers with a 10-km width (Ledwell et al. 1993) and are characterized with very much weaker dynamical anomalies.

The motivation to focus on the vertical exchanges of tracers associated with mesoscale and submesoscale structures is that the concentrations of many oceanic tracers, such as temperature, salinity, nutrients, dissolved oxygen, and dissolved organic and inorganic carbon, change rapidly with depth just below the mixed layer. These substances are indeed typically forced or modified either in the upper ocean or at the air-sea interface by processes such as biological production and air-sea exchanges, but their vertical exchanges with the deep interior occur at much lower rates. Over long timescales, the mean vertical concentration profiles of these substances are set by the balance between their rate of production or removal in the upper ocean, the rate of vertical exchanges between the upper ocean and the interior, and their replenishment in the interior by large-scale advection and biogeochemical reactions.

The vertical exchanges of waters between the upper ocean and the interior usually occur both within and below the mixed layer. However, except during the wintertime convection when the mixed layer deepens significantly, the vertical velocity within the mixed layer that is principally wind-driven does not affect the exchanges between the surface layers and the ocean interior very much (Haine & Marshall 1998, Giordani & Caniaux 2005). These exchanges are therefore driven mostly by the vertical velocity below the mixed layer, where the tracer vertical gradients are very much larger than in the mixed layer, and this vertical velocity is captured entirely by the mesoscale

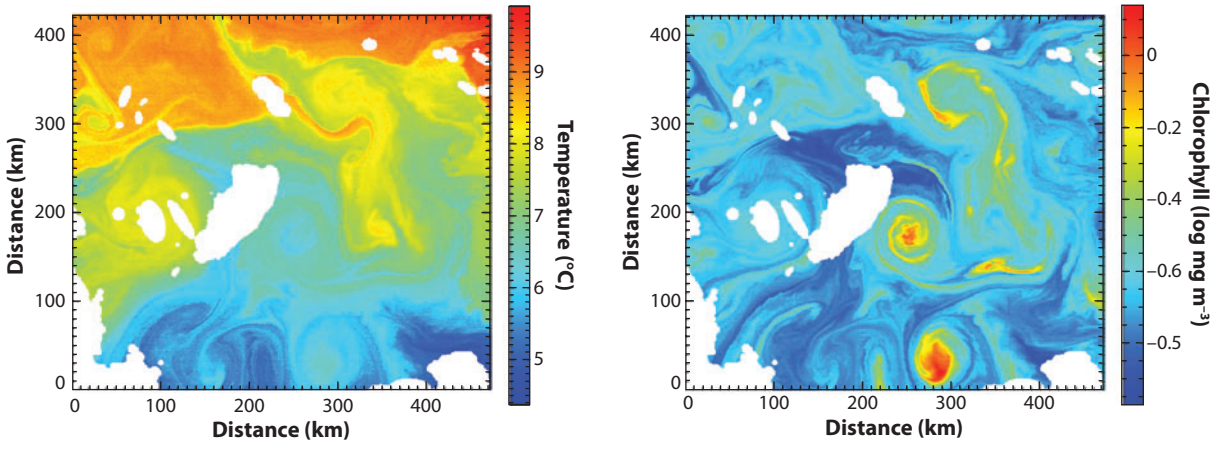

Figure 1

Sea surface temperature (*left*) and ocean color images (*right*) from satellite data (courtesy of Jordi Isern-Fontanet).

and submesoscale dynamics (Spall 1995, Nurser & Zhang 2000, Lapeyre et al. 2006, Capet et al. 2008b).

Biogeochemists such as Jenkins (1988) have brought the relative importance of vertical exchanges of tracers due to mesoscale eddies to the forefront. Indeed, global biogeochemical estimates indicate that nutrient supply by mesoscale eddies represents a significant part of the annual nutrient requirement (McGillicuddy et al. 2003), but this part still appears to be underestimated (McGillicuddy et al. 2007). Geochemical estimates of new production well surpass the apparent rate of nutrient supply by winter convection by a factor of two and the estimated mesoscale eddy nutrient injection accounts for only 20–30% of this annual requirement (McGillicuddy et al. 2003, 2007). This discrepancy has motivated a large number of studies devoted to this problem (Garçon et al. 2001, McGillicuddy et al. 2007, Lévy 2008) and stimulates the ongoing vivid debate among biogeochemists about what missed physical mechanisms could close the nutrient budget through additional vertical nutrient supply (McGillicuddy et al. 2007). The most believable mechanism seems to be related to the underestimation of the dynamics at small scale because of the lack of resolution, which is strikingly apparent when one considers the ocean color signal and its spatial variability. Through the use of very high-resolution satellite imagery, researchers recognized that the submesoscales account for approximately 50% of the total resolved variance (Glover et al. 2008). Such high variance highlights the issue of the vertical nutrient supply at small scale.

Conversely, fluid dynamicists have obtained a wealth of results in the past decade on the impact of the small-scale dynamics on a turbulent eddy field. These results significantly strengthen the vision of an upper ocean crowded with a large number of strongly interacting eddies. Numerical experiments in the North Atlantic basin (Hurlburt & Hogan 2000, Siegel et al. 2001) have shown that a horizontal resolution of 1.5 km leads to an explosion of eddies and to an eddy kinetic energy increase by a factor of ten compared with eddy resolving simulations (15-km resolution). More recent numerical simulations of ocean dynamics (Capet et al. 2008a, Klein et al. 2008), with very high resolution both in the horizontal and in the vertical, were carried out to fully resolve the stratified mesoscale and submesoscale eddy turbulence. These studies further highlight the impact of the dynamics of small scales on the vertical exchanges: The vertical velocity variance increases by a factor of ten when the resolution increases from 6 km to 1 km (Klein et al. 2008).

We first review the numerous biogeochemical studies devoted to the vertical exchanges of tracers due to eddies. We focus on what is known and the remaining uncertainties and problems about the role of the small scales because of the lack of spatial resolution. Conversely, results from dynamical studies—both theoretical and numerical—may help to answer the questions from biogeochemical studies. We then review their main findings with a particular focus on the vertical pump associated with mesoscale turbulence.

CONCEPTUAL VIEWS OF THE VERTICAL EXCHANGE OF TRACERS FROM BIOGEOCHEMICAL STUDIES

In the past 20 years, a large number of studies has been undertaken to quantify the vertical exchanges of tracers driven by mesoscale eddies. Most of these studies focused on biogeochemical issues. Their purpose was to address the crucial question of what missed physical mechanisms could close the budget of phytoplankton production through additional nutrient supply (Jenkins 1988). These studies include field experiments, realistic numerical simulations at a basin scale, analysis of satellite data, and academic studies. Many of these studies are detailed in Garçon et al. (2001), Martin (2003), and Lévy (2008). Some new answers have been obtained, but important questions remain.

Two conceptual views emerge from these studies. The first view consists of directly relating the time evolution of the eddy anomaly to the vertical transport (through a linear relationship), which implicitly assumes that the vertical exchanges occur principally in the interior of mesoscale eddies. This view includes the eddy pumping paradigm. The second view points out the possibility of vertical pumping directly at small scales, i.e. within the submesoscale structures, through frontal and strongly ageostrophic processes. In this scenario the mesoscale eddies contribute indirectly to the vertical transport because submesoscale structures (such as filaments in the close vicinity or far off of the eddies) are produced by the mesoscale eddy-eddy interactions.

Vertical Exchanges in the Interior of Mesoscale Eddies

Most studies (in situ experiments, numerical modeling, or satellite data analysis) that aim to understand and quantify the vertical exchange of biogeochemical tracers have focused on the interior of mesoscale eddies. The main reasons for this approach are that observable dynamical anomalies—SSH, density, horizontal currents—have much larger amplitudes within these eddy structures than outside or between them. Furthermore, because these eddies capture most of the kinetic energy or the density variance signals, the vertical kinetic energy signal is commonly believed to be strongly tied to them as well. A typical example to motivate this belief is the Ekman pumping mechanism, for which the vertical velocity near the surface is proportional to the geostrophic vorticity (Martin & Richards 2001), and hence assumed to be maximum at the center of an eddy (negative for a cyclone and positive for an anticyclone). A similar eddy/wind interaction was invoked recently (McGillicuddy et al. 2007).

Vertical velocities associated with mesoscale eddies are difficult to measure directly because they are typically orders of magnitude smaller than the horizontal velocity (1 mm/s versus 20 cm/s). Indirect diagnostics through the Omega equation (as discussed in the section on The Turbulent Eddy Regimes and the Associated Vertical Pump) necessitate very good sampling and well-resolved synopticity that are rarely met in mesoscale eddies (Allen et al. 2001, Martin & Richards 2001). To circumvent these limitations, McGillicuddy & Robinson (1997) and McGillicuddy and coworkers (1998), using results from the Bermuda Testbed Mooring (McNeil et al. 1999), have proposed an indirect estimation of the vertical fluxes of tracers using the eddy pumping mechanism (see **Figure 2**). The basic argument is that the vertical velocity at a given level is related to the density time evolution, e.g.,

$$w = \frac{g}{\rho_0 N^2}\left(\frac{\partial \rho}{\partial t} + \vec{u}\cdot\nabla\rho\right). \quad (1)$$

If a surface cyclone (associated with a positive density anomaly) strengthens or an anticyclone (negative density anomaly) decays, then through this equation one can expect a positive vertical velocity inside the eddy. A negative vertical velocity would occur in the case of the decay of the cyclone. The role of the eddy pumping of nutrients in cyclonic eddies has been investigated in several other studies that used moored instrumentations and shipboard surveys, either in the North Pacific (Falkowski et al. 1991, Allen et al. 1996) or the North Atlantic (Robinson et al. 1993, McGillicuddy et al. 1999). These studies confirmed that high primary production could be observed in the eddy interior in agreement with the eddy pumping mechanism.

This eddy pumping paradigm was used in other studies to attempt to estimate global nutrient fluxes (Siegel et al. 1999, Martin & Pondaven 2003). In particular, Siegel and coworkers (1999) combined altimeter data and a simple nitrate-density relationship deduced from Bermuda Atlantic Time-series Study (BATS) data to remotely estimate upper ocean isopycnal displacements and the nitrate flux into the euphotic zone due to eddy pumping. However, even if the direct relationship

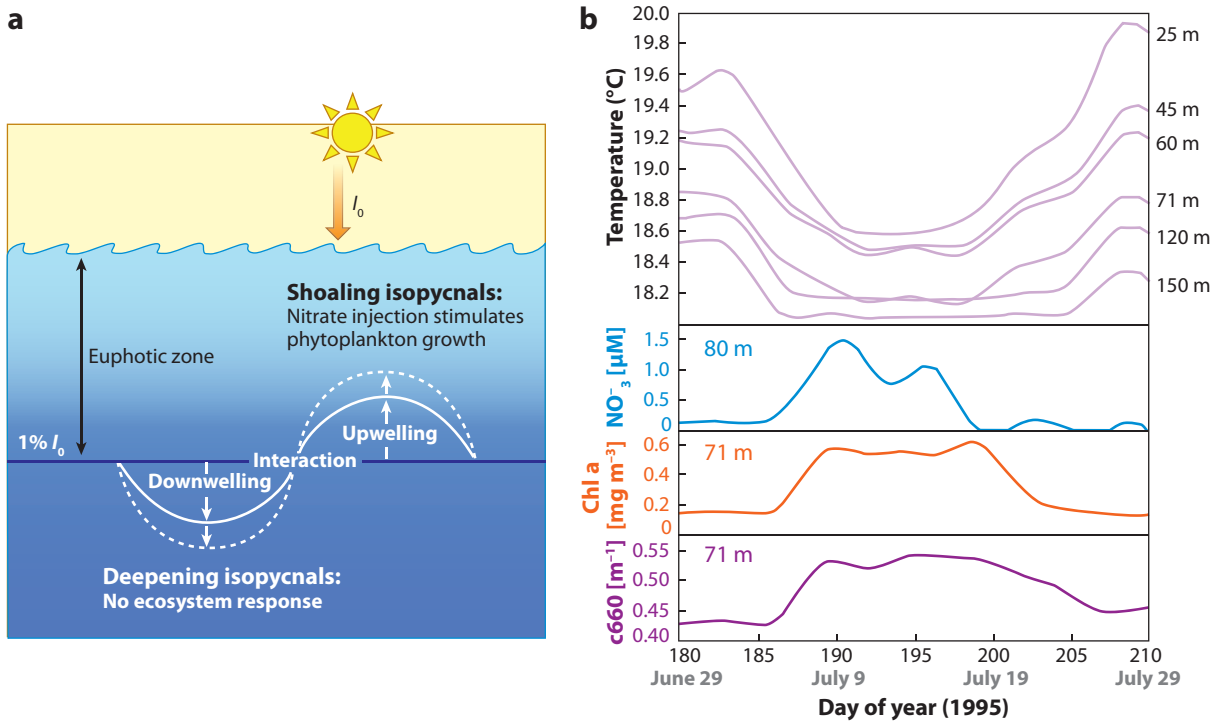

Figure 2

(*a*) Schematic representation of the eddy-induced upwelling mechanism. (*b*) Results from the Bermuda Testbed Mooring third deployment during the summer of 1995. Modified with permission from Macmillan Publishers Ltd.: *Nature*, McGillicuddy et al. (1998).

between nitrate and density seems to be the case at the mesoscale, the correlation of ocean color and sea surface temperature patterns seems to be weak at smaller scales (McGillicuddy et al. 2001).

Realistic coupled physical-biogeochemical numerical simulations at a basin scale (Oschlies & Garçon 1998; Oschlies 2002a,b; McGillicuddy et al. 2003) have implicitly endorsed the eddy pumping paradigm. Some simulations such as that of Oschlies & Garçon (1998) assimilate altimeter data to closely reproduce eddy activity in the models. Nutrient isolines below the euphotic zone mostly follow the isopycnals either because of the low resolution [1/3° in Oschlies & Garçon (1998)] or because of a first-order relaxation using a reference nutrient-density relationship and the modeled density such as that in the 1/10° degree resolution study of McGillicuddy et al. (2003).

These coupled physical-biogeochemical numerical simulations [starting with that of Oschlies & Garçon (1998)] have produced important breakthroughs by providing a totally different vision of the nitrate budgets and the annual new production at a basin scale. In the coarse resolution model (2°) of Fasham and coworkers (1993), the main sources of nitrate at the BATS site were the horizontal advection and the winter convection. Ten years later, McGillicuddy and colleagues (2003), using an eddy-resolving model (1/10°), show that the main sources of nitrate at the same site are the vertical advection due to the mesoscale eddies and the winter convection. Above all, these studies point out the issue of spatial resolution for the mesoscale eddy contributions. The eddy-permitting simulation of Oschlies (2002a,b), which uses a 1/3° degree horizontal resolution, indicates that the contribution of the mesoscale eddies in the vertical advection of nitrate is entirely canceled out by the Ekman downwelling contribution (driven by the wind-stress curl). However, the eddy-resolving simulations (1/10°) of McGillicuddy and coworkers (2003) reveal that the

contribution of mesoscale eddies far surpasses that of the Ekman downwelling contribution, such that the total vertical advection of nitrate is now significantly positive. McGillicuddy and coworkers (2003) found that 20% to 30% of the total vertical fluxes of nitrate is explained by the mesoscale eddies. Such an impact of the spatial resolution was also addressed by Mahadevan & Archer (2000). These authors explore the range of resolution from 40 km to 10 km in a coupled physical-biogeochemical model. They show a tremendous increase of the primary production (up to a factor of three) in response to a resolution increase from 40 km to 10 km. This increase was shown to be entirely due to a much better representation of the vertical advection of nutrients by mesoscale eddies. All these studies, however, do not indicate that a convergence (related to the spatial resolution) has been attained.

Satellite data such as those for SST and ocean color (mostly related to the phytoplankton concentration) have an horizontal resolution (approximately 1 km) that is much higher than that of the in situ data, the altimeter data, or the preceding basin-scale biogeochemical models. These data reveal not only a large number of mesoscale eddies, but also the presence of numerous submesoscale structures, such as thin filaments with a width equal to or less than 10 km, located in the vicinity of or far off of the eddies (e.g., Gower et al. 1980). But in terms of the vertical pump, biogeochemical studies related to high-resolution satellite images explicitly or implicitly assume that most of the tracer vertical injection within the upper layers occurs either at much larger scales [because of a strong wind event that deepens the oceanic mixed layer on a scale of O(1000 km) as in Abraham (1998)] or within the mesoscale eddies (Lehahn et al. 2007). The emergence of the submesoscale structures is then usually interpreted (Abraham 1998, Abraham et al. 2000, López et al. 2001, Abraham & Bowen 2002, Martin 2003, Lehahn et al. 2007) in terms of horizontal dispersion driven by the two-dimensional turbulence dynamics (see section on The Turbulent Eddy Regimes and the Associated Vertical Pump) and therefore with no impact on the vertical exchanges.

This conceptual view, which implicitly assumes that the vertical exchanges occur principally in the interior of mesoscale eddies, has contributed to significant advances for the estimation of the vertical exchanges due to mesoscale eddies. But this view is based on assumptions whose questioning may help to improve this estimation. First, this view implicitly assumes that nutrients or tracers are well mixed on isopycnals. Second, this view assumes that the space between the mesoscale eddies is a dynamical desert in terms of the vertical pump.

Vertical Exchanges in the Submesoscale Structures

The impact of the submesoscale structures (including filaments in the close periphery or far off of the mesoscale eddies) on the vertical exchanges has been addressed by another class of studies. A large number of these studies [such as those of Spall & Richards (2000), Lévy et al. (2001), Mahadevan & Campbell (2002), and Martin et al. (2002)] proposes a vision radically different from the studies described in the preceding section.

To discriminate between the different types of vertical exchanges (at mesoscale, submesoscale, or large scales), an understanding of the vertical velocity field is required. One solution to estimate the vertical velocity in mesoscale surveys is to measure the three-dimensional density and horizontal velocity fields [using for example Seasor and acoustic Doppler current profiler (ADCP) instruments; Rudnick 1996, 2001; Shearman et al. 1999] and to retrieve the vertical velocity by using the classical Omega equation (Hoskins et al. 1978), which reads

$$N^2\nabla^2 w + f^2 w_{zz} = -2\frac{g}{\rho_0}\nabla\cdot\vec{Q}, \qquad (2)$$

where $\vec{Q} = -[\nabla \vec{u}]^{\mathrm{T}} \nabla \rho$ is the Q-vector (Hoskins et al. 1978). This methodology [see also Viudez & Dritschel (2004)] was developed in the atmospheric community to study balanced motions associated with fronts but it is valid in most situations (including the ocean), even with high Rossby number. This methodology is employed in the majority of oceanic field studies (Tintoré et al. 1991; Pollard & Regier 1992; Rudnick 1996; Shearman et al. 1999; Allen et al. 2001, 2005; Martin & Richards 2001).

One problem with computing w from Equation 2 is the availability of high-resolution data, in particular within mesoscale eddies, even if the amplitudes of the dynamical anomalies are large there. Allen and coworkers (2001) and Martin & Richards (2001) address this issue and show that significant errors in the accuracy of vertical velocities arise from the necessary compromise between the spatial resolution and synopticity of a hydrographic survey. Martin & Richards (2001), when investigating the vertical transport processes that produce a source of nutrients within an anticyclonic eddy, further point out the constraints due to the sampling strategy. These researchers show that observations on an unequally horizontally spaced grid produce an artificial distortion of the vertical velocity field. Thus, a survey track spacing (using Seasor and ADCP instruments) inside a circular eddy, involving high-resolution (2 km) zonal sections, 20 km apart, leads to strong artificial north-south alignment of up/downwelling regions (**Figure 3**). Interpolation of the same data on an equally spaced grid [as in Shearman et al. (1999)] provides a more believable w field but degrades the resolution and leads to a significant underestimate of this field as noted by Martin

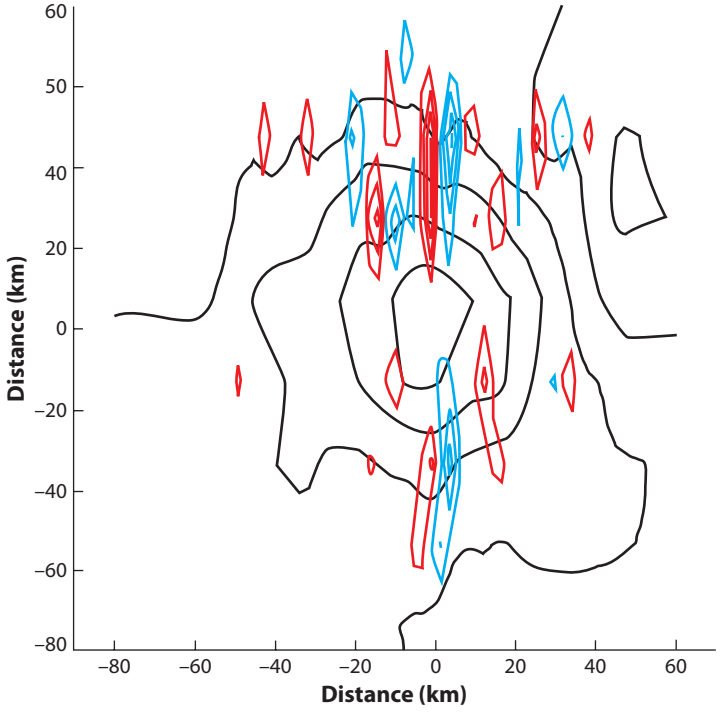

Figure 3

Geopotential (*circular contours in black*) and vertical velocities (*elongated contours in color*) at 72 m. Upward velocities are red, downward velocities are blue. Velocity contour intervals are 5 m per day. The strong north-south alignment of up/downwelling regions is an artifact due to the survey track spacing. Adapted from Martin & Richards (2001) with permission from Elsevier.

& Richards (2001). This result indicates that the w field within mesoscale eddies is small scale and that the lack of spatial resolution makes a reliable estimation of this w field, on a global scale, almost impossible to obtain.

Surveys of elongated density fronts are much easier than surveys of fronts associated with almost circular eddies because high-resolution sampling can be assigned mostly on the cross-front direction (Pollard & Regier 1990, 1992; Tintoré et al. 1991; Allen & Smeed 1996; Allen et al. 2005; Rudnick 1996). Pollard & Regier (1992) used high-resolution sampling across a density front to produce estimations of 40 m/day at 200 m. This order of magnitude of the vertical velocity field was found in small-scale structures by Legal and coworkers (2007) using data obtained from a high-resolution survey located in a region between eddies where the density anomalies were quite weak. Their results revealed a vertical velocity field far-off eddies with amplitudes of up to 30 m per day at a 200-m depth within elongated thin filaments, less than 10-km wide and with weak density anomalies [which actually led to density fronts with approximately the same strength as in Pollard & Regier (1992)].

Studies such as that of Strass (1992) have shown that high chlorophyll could be observed outside the eddies, in frontal regions at submesoscale (**Figure 4**). This result is indeed coherent with the Omega equation because vertical velocities will be observed on each side of the density front and

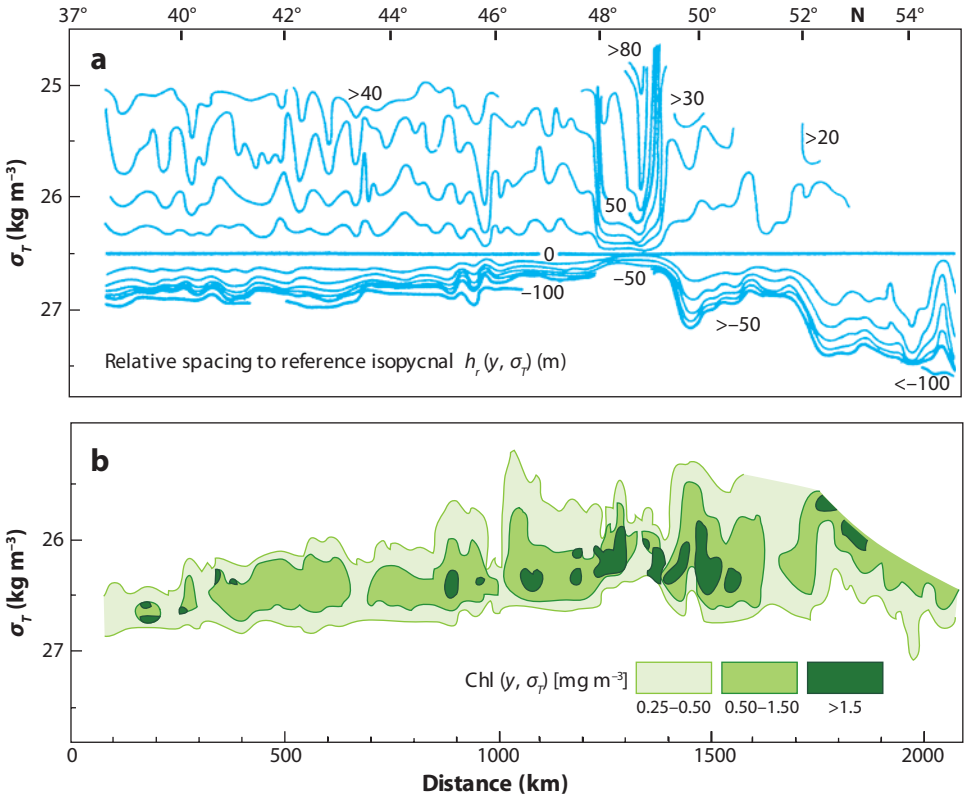

Figure 4

Isopycnal distributions along a section from the Azores toward Cape Farvel, Greenland of (*a*) the spacing of isopycnals relative to 26.5 kg m^{-3}, and (*b*) the chlorophyll concentration. High chlorophyll concentrations are observed in submesoscale fronts. Redrawn from Strass (1992) with permission from Elsevier.

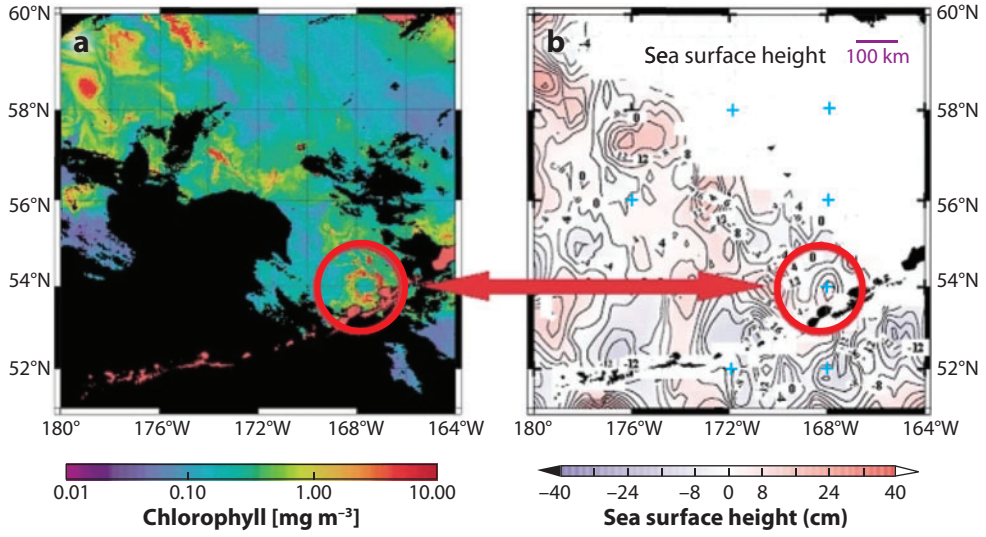

Figure 5

Observations of (*a*) chlorophyll concentration and (*b*) sea surface height in the Bering Sea. The red circles show an anticyclonic structure. Adapted from Mizobata et al. (2002) with permission from Elsevier.

tend to flatten the isopycnals (**Figure 9*a***). Looking at an eddy as a front in its radial direction, we conclude that the vertical exchanges should be mostly efficient on the periphery of the eddy and not on the center, as in the eddy pumping view. Indeed, Lima and coworkers (2002), Mizobata and coworkers (2002), and Stapleton and coworkers (2002) have found chlorophyll just at the periphery of eddies in ocean color data (**Figure 5**).

This radically different vision of vertical injection, involving small-scale fronts, is endorsed by several numerical studies (such as those of Macvean & Woods 1980, Spall 1995, Haine & Marshall 1998, Nurser & Zhang 2000, Spall & Richards 2000, Lévy et al. 2001, Mahadevan & Campbell 2002, Martin et al. 2002). In particular, the question of the existence of small-scale upwellings and downwellings (versus large-scale) within a turbulent eddy field has been addressed by Lévy and coworkers (2001). They show that using a higher spatial resolution (2 km instead of 6 km) produces very different w structures. High resolution leads to w structures with much smaller scales and a much larger amplitude, and characterized by either multipolar hot spots of large vertical fluxes or thin elongated patterns both within and outside the eddies (**Figure 6**).

Furthermore, these researchers found that considering these small-scale w structures (by increasing the numerical resolution from 6 km to 2 km) leads to an increase in the vertical velocity variance by a factor of three and double the primary production and the phytoplankton subduction. Finally, a very significant part of this increase is due to the small-scale hot spots of upwellings located within submesoscale structures, such as filaments located outside the eddy cores (Lévy et al. 2001).

Mahadevan & Campbell (2002) analyze a situation where first, upwelling of tracers from deeper layers into upper layers occurs at small scale and second, sources or sinks of tracers within the upper layers differ from those for density. These researchers show that the patchiness of tracers in these upper layers results from the competition between these small-scale vertical tracer fluxes and the timescale of their removal by sinks (such as primary production for nutrients). Their conclusions point out the important role of these sinks and sources and their time rates, and interestingly

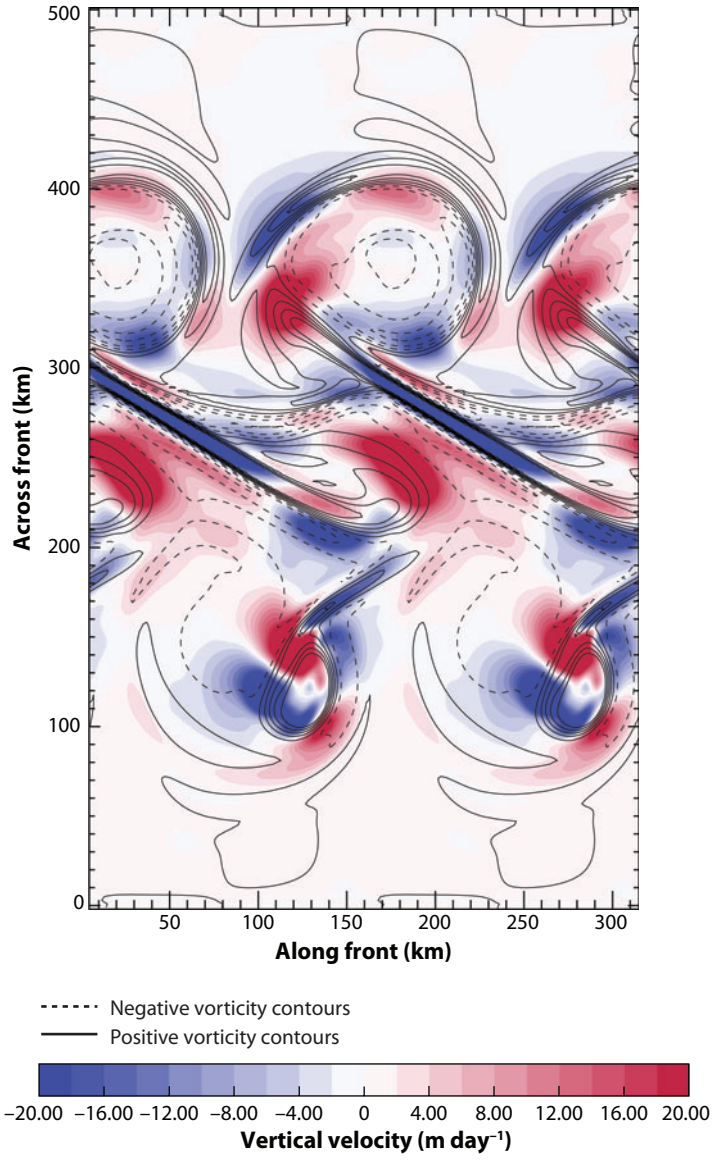

Figure 6

Vertical velocities at 90 m (*red for upward and blue for downward*). Adapted with permission from primitive equation simulations described in Lévy et al. (2001).

oppose the results of Abraham (1998) that considered large-scale vertical injection of tracer [see Martin (2003) and Lévy (2008) for a detailed discussion of Abraham's (1998) results]. Indeed, when the removal rate of tracer within the upper layers is large, the resulting tracer horizontal heterogeneity displays a much shallower spectral slope than when this rate is small. The study of Mahadevan & Campbell (2002) clearly points out [in somewhat the same way as Abraham (1998)] that the spatial heterogeneity of SST (or density) and tracer anomalies should be different if their sinks and sources are different. This result [confirmed by Lévy & Klein (2004) in more realistic physical-biogeochemical simulations] apparently contradicts the eddy pumping paradigm invoked

by other studies that assumes tracers are well-mixed over isopycnals, and indicates that tracers, depending on their removal rate, mark out the stages of an inverse cascade through time.

Martin and coworkers (2002) addressed the question of the impact of small-scale versus large-scale upwellings of chemical tracers from deeper layers into the upper layer. They show that numerous small-scale upwelling regions increase the primary production by 140% compared with when one large-scale upwelling hot spot is considered, even if the total rate of upwelling is constant for the two cases. Furthermore, sinks of nutrients (induced by primary production) are much more efficient when small-scale upwelling hot spots are considered. The magnitude of this discrepancy is furthermore influenced by the presence of mesoscale eddies. Indeed, Martin and coworkers (2002) found that this magnitude increases by 30% when small-scale hot spots of upwelling are localized evenly within or outside the eddy cores compared with when they are localized only within the core of mesoscale eddies.

Impact of the Spatial Resolution?

The image that seems to emerge so far from biogeochemical studies devoted to the vertical exchanges of tracers induced by oceanic eddy turbulence, using in situ data, is that these exchanges are mostly located within mesoscale eddies. The arguments that explain this image rely less on dynamical reasons than on the fact that observations mostly concern mesoscale eddies, where the amplitude of dynamical anomalies is large and therefore much more easily observable. Furthermore, the nutrient-density relationship proposed to circumvent the constraints related to the sampling strategy (or the lack of spatial resolution) implicitly focuses on mesoscale eddies (where density anomalies are large) and excludes a priori any impact of the small scales on the vertical pump. These results suggest that the remaining space, between the eddies where the amplitude of density anomalies is much smaller, is a dynamical desert in terms of vertical fluxes of any tracer.

Still, a very large number of small-scale structures, even in chlorophyll, is observed between the eddies on high-resolution satellite images. But they are usually interpreted solely in terms of horizontal dispersion by oceanic eddies, because the vertical injection of tracers is again assumed to be either large scale or within the mesoscale eddies.

However, this weak impact of the small scales on the vertical exchanges of tracers is strongly questioned by fine-scale studies. These studies suggest that when the spatial resolution is high enough, much larger vertical exchanges of tracers are obtained and this significant increase is principally due to the small scales. Furthermore, these studies point out that the existence of small-scale upwelling or downwelling hot spots and their location relative to the mesoscale eddies may have a significant impact on the bioreaction of the tracers at a global scale.

To better understand the role of these small scales on the vertical exchanges of tracer, one must turn to dynamical studies that have examined the three-dimensional characteristics of these small scales and their relation to the turbulent eddy field.

THE TURBULENT EDDY REGIMES AND THE ASSOCIATED VERTICAL PUMP (FROM DYNAMICAL STUDIES)

Dynamical studies, in particular those of the past decade, help to unveil the physical processes missed by the preceding biogeochemical studies, and in particular may help us understand the dynamical importance of the small scales on the vertical exchanges of tracers associated with a turbulent oceanic mesoscale eddy field. Studies based on a geophysical fluid dynamics approach highlight the existence of two distinct turbulent regimes appropriate for stratified rotating flows. The first regime is driven by interior potential vorticity anomalies that result from nonlinear

baroclinic instability. This regime focuses on the dynamics in the ocean interior (Rhines 1983; Hua & Haidvogel 1986; McWilliams 1989, 1990; Smith & Vallis 2001, 2002). The second regime is driven by surface density anomalies and takes into account surface frontogenesis. This regime is described by the surface quasigeostrophic (SQG) model (Held et al. 1995) and is known to be pertinent to characterize the dynamics near vertical boundaries, such as the upper troposphere (Juckes 1994, Tulloch & Smith 2006) or the upper ocean (Isern-Fontanet et al. 2006a, LaCasce & Mahadevan 2006, Lapeyre & Klein 2006b). These two turbulent regimes have very different properties, in particular for vertical transport, as detailed below. Subsequent studies (Lapeyre & Klein 2006a; Klein et al. 2008; R. Tulloch & K.S. Smith, manuscript submitted) have begun to reveal which regime applies to the dynamics of the upper oceanic layers and the level of scale dependence. Some issues remain to be examined, in particular about the interaction between the two types of dynamics, but the results already obtained may help to answer questions from the biogeochemical studies and inspire future studies.

Some Basic Properties

Before reviewing these dynamical studies, it is useful to briefly recall some definitions and basic properties. The flow associated with a turbulent oceanic eddy field within a stably stratified fluid is weakly dissipative and horizontal motions are approximately geostrophic owing to the influence of the rotation of the Earth. These characteristics are described by the following three nondimensional parameters: a large Reynolds number ($Re = UL/\nu \gg 1$), a small Rossby number ($Ro = U/f_0 L \leq 1$), and a Burger number $B = \lambda^{-2}/L^2$ close to one. The velocity scale (U) is of the order of 0.1 m $\times$ s^{-1}, $L \approx 100$ km is the length scale of the mesoscale eddies, and ν is the viscosity. $f_0 \approx 10^{-4}$ s^{-1} is the Coriolis parameter for mid-latitudes and $\lambda^{-1} = NH/f_0$ is the first Rossby radius of deformation (where $H \approx 2000$ m is the depth scale of eddies and N is the Brunt-Väisälä frequency).

In this parameter space, the time evolution of a mesoscale eddy field in quasigeostrophy theory (Charney 1971, Pedlosky 1987) is governed by the conservation of the potential vorticity (PV) in the ocean interior,

$$\frac{d}{dt}\left(\nabla^2\psi - \frac{gf_0}{\rho_0}\frac{\partial}{\partial z}\left(\frac{\rho}{N^2}\right)\right) = 0, \tag{3}$$

associated with the conservation of density at the surface,

$$\frac{d}{dt}\rho(z=0) = 0. \tag{4}$$

The PV equation involves relative vorticity ($\zeta = \nabla^2\psi$) and a vortex stretching term. Basic properties of the geostrophic turbulence are detailed in many reviews (see for example those by Rhines 1979 and McWilliams 1990) and in the textbooks of Pedlosky (1987), Vallis (2006), and McWilliams (2006).

One important property of an eddy field is that it can stir horizontally any passive or active tracer such as potential vorticity [first seen by Welander (1955) in the oceanographic community]. The geometry of the stream function field (deduced from the horizontal motions) involves elliptical (or circular) and hyperbolical flow structures (Weiss 1991). This phenomenon is due to the action of both the deformation part of the velocity field (also called the strain field), which permanently stretches and expands any patch of tracer, and the vorticity part, which tends to fold any patch of tracer. In elliptical regions, for example inside mesoscale eddies where the relative vorticity dominates over the strain, any tracer pattern is weakly deformed. Hyperbolical structures are deformation regions where the strain dominates. In these regions any tracer pattern

is horizontally stretched into elongated and thin filaments. Several criteria have been proposed and used to partition such a turbulent eddy field into elliptic and hyperbolic regions (Weiss 1991, McWilliams 1984, Hua & Klein 1998, Lapeyre et al. 1999, Klein et al. 2000). In particular, Lapeyre et al. (1999) and Klein et al. (2000) detail the characterization of the orientation of the tracer fronts and their time evolution.

The basic properties of the nonlinear interactions between eddies are well described by two-dimensional turbulence studies (see McWilliams 1990 for a review). Classically, one particular circular eddy can be stretched by the deformation field of nearby eddies (McWilliams 1984). If the deformation field is strong enough, this eddy (and therefore its relative vorticity) may be irreversibly stretched into filaments; these filaments are advected far away by the exterior flow or merge with the vorticity of eddies of the same sign if the latter are close enough. If the deformation field is weaker, the eddy recovers a circular shape, with a steeper vorticity profile near its edge, by expelling relative vorticity from the outer edges of the ellipse (Mariotti et al. 1994). This steep vorticity profile acts as a dynamical barrier that prevents further stretching of the eddy by the deformation field of other eddies (Mariotti et al. 1994).

The Regime of Interior Quasigeostrophic Turbulence

The study of divergent flows requires a consideration of the full expression of the potential vorticity, i.e., including the vortex stretching term. The interior quasigeostrophic (QG) turbulent regime is based on a small Rossby number approximation (Charney 1971, Rhines 1979). This regime further assumes that motions are not influenced by vertical boundary conditions on the streamfunction and behave as though these conditions were homogeneous (Charney 1971). Consequently, surface density anomalies are assumed to be zero. Depth dependence of the related motions can then be understood within the framework of the normal mode analysis detailed in Gill (1984). Motions are expanded in terms of a barotropic mode and baroclinic modes (Fu & Flierl 1980). Increasing the spatial resolution in the three directions does not change significantly the properties highlighted by these turbulence studies (McWilliams 1989, Smith & Vallis 2001). These properties include a steep velocity spectrum (close to k^{-3} or k^{-4}), a direct cascade of baroclinic (or potential) energy from large to small scales, and an inverse barotropic energy cascade from scales close to the Rossby radius of deformation to larger scales (Salmon 1980, Hua & Haidvogel 1986, Held & Larichev 1996, Smith & Vallis 2002). This phenomenon is accompanied in physical space by eddies that become larger and larger through vortex mergers.

To study the basic properties of such a divergent flow, Larichev & McWilliams (1991) use the equivalent barotropic model that mimics the behavior of a single baroclinic mode. The vortex stretching term is equal to $\lambda^2\phi$, where λ^{-1} is the Rossby radius of deformation of the baroclinic mode and ϕ is the stream function. Such a model is consistent with the findings of Smith & Vallis (2001), who showed that surface-intensified stratification slows the transition from the baroclinic mode to the barotropic mode, so the energy of the upper ocean concentrates in the first baroclinic mode. Polvani and coworkers (1994) extended the results of Larichev & McWilliams (1991) to Rossby number of order one by using a shallow-water model. Both Larichev & McWilliams (1991) and Polvani and coworkers (1994) indicate that including a nonzero stretching term (and therefore a nonzero vertical velocity field or vertical pump) has profound impacts on the dynamics of the nonlinear interactions and the equilibrium of the eddy field compared with the two-dimensional barotropic turbulence case. First, the inverse kinetic energy cascade is significantly slowed down (Larichev & McWilliams 1991). Indeed, the timescale associated with these features is given by

$$t_\lambda = \langle \zeta^2 \rangle^{-1/2} [1 + \lambda^2/\bar{k}^2],$$

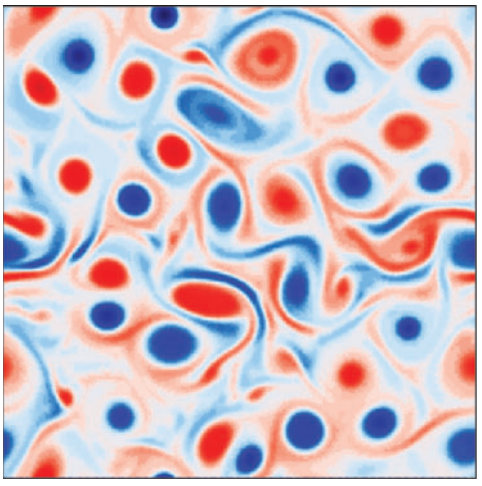

Figure 7

Relative vorticity field in the interior quasigeostrophic (QG) regime: vortices are weakly interacting. Reprinted with permission from Polvani et al. (1994). Copyright 1994, American Institute of Physics.

where $\bar{k}$ is the centroid wavenumber for the kinetic energy spectrum. This timescale describes the rapidity and the efficiency of the eddy-eddy interaction. McWilliams (1984) showed that for barotropic turbulence ($\lambda = 0$) or two dimensional turbulence, these interactions are strong because t_λ is small. Here, for the ocean interior, $\bar{k}$ is usually equal to or smaller than λ, which means larger t_λ and therefore a slowing of the inverse cascade and of the interactions by a factor equal to or larger than two, with the following characteristics: Mesoscale eddies in such a flow are either separate or partly joined with another of the same sign, or more rarely are paired with another of opposite sign. The partial joining of like-sign eddies is a middle stage of vortex merger before they become a composite monopole. Merging in such a flow actually has the appearance of cell mitosis in backward time (Larichev & McWilliams 1991). This phenomenon is in strong contrast to the merging dynamics in pure two-dimensional turbulence that involve vigorous ejection and winding up of vorticity filaments [as illustrated in McWilliams (1984)]. Furthermore, unlike what happens in two-dimensional turbulence, the eddies do not move far from their initial positions, they move only to a distance that is on the order of an eddy radius. After the eddies have grown to a size comparable to λ^{-1}, they are in the quasi-equilibrium phase (Larichev & McWilliams 1991, Polvani et al. 1994) and interact only weakly (**Figure 7**). Thus, the production of submesoscale structures, i.e., filamentation, is much less efficient with such divergent flows than in two dimensional turbulence.

The vertical velocity field is located mostly within the mesoscale eddies because large vorticity amplitudes are found principally in the eddy cores. One major result for this regime is that when the Rossby number is of order one, anticyclonic structures dominate over cyclonic structures (Polvani et al. 1994).

The Surface Quasigeostrophic Turbulent Regime

Another class of divergent flows is used principally to describe the oceanic mesoscale eddy field in the surface layers. This class is based on the SQG equations or their extension to Rossby number of order one (see Muraki et al. 1999 and Hakim et al. 2002, for details). This class was first introduced by Blumen (1978) and was subsequently described by Held et al. (1995) and Hakim et al. (2002).

The SQG model is a reduction of the Eady model to just one boundary (for example, the ocean surface). Essentially, the surface density is a Dirac delta function of potential vorticity, as first recognized by Bretherton (1966). One important property is that surface density anomalies are nonzero and are stirred by mesoscale eddies, which leads to strong density gradients at submesoscale (in a process called frontogenesis), with significant consequences for the turbulence dynamics.

In SQG divergent flows, the potential vorticity is assumed to be uniform and constant and the dynamics is driven by the time evolution of the density at the surface. One first major distinction from the interior QG regime is that horizontal motions at small-scale are much more energetic: The velocity spectrum has a $k^{-5/3}$ slope (Pierrehumbert et al. 1994, Held et al. 1995), instead of k^{-3} or k^{-4} for the preceding flows. Furthermore, the relative vorticity spectrum has a $k^{1/3}$ slope, which means that large vorticity amplitudes are now found within the submesoscale structures. A dynamical explanation, noted by Held and coworkers (1995), is that whereas the density at the surface is conserved on a Lagrangian trajectory, the horizontal density gradient increases exponentially as the scale of the structure decreases because of the stirring processes. At the same time, the associated relative vorticity increases because it is proportional to the density gradient (due to the uniformity of PV). Finally, Held and coworkers (1995) note that the exponential increase of the relative vorticity in small-scale structures is large enough to overcome the strain stabilization effects (Waugh & Dritschel 1991) and leads to shear instability and to the formation of small-scale coherent vortices that subsequently merge to form larger eddies.

On a global scale, the inverse cascade of surface kinetic energy in SQG (Capet et al. 2008c) displays properties somewhat different from two-dimensional and interior QG turbulence (**Figure 8**). SQG inverse cascade is far more intense than for the previous turbulent regimes. Held and coworkers (1995) and Hakim and coworkers (2002) note that, unlike these previous regimes, there is a considerable pairing of eddies with opposite sign that form dipoles. These dipoles quickly propagate until they collide with a third eddy. Eddy encounters are far more violent than in two-dimensional flows and are accompanied by the production of a much larger number of filaments (Lapeyre & Klein 2006b). Another difference is that filament instabilities, mentioned above, produce small-scale satellite eddies, which further feed the inverse kinetic energy cascade near the surface.

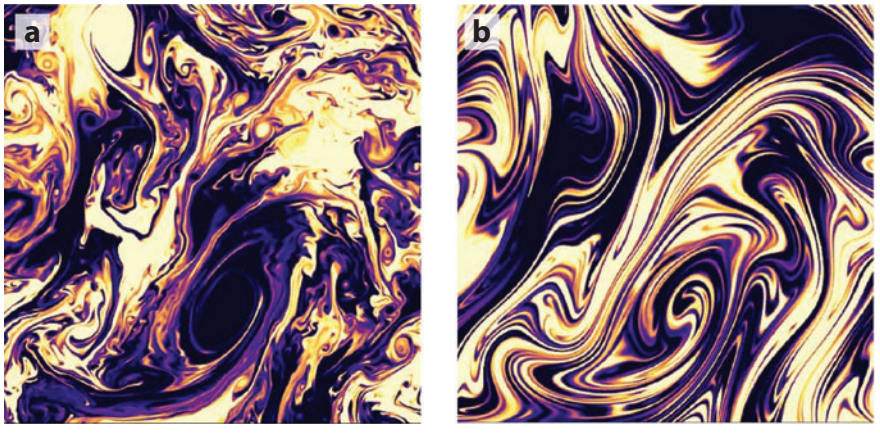

Figure 8

Snapshot of passive scalar fields in a region (*a*) driven by the surface quasigeostrophic (SQG) regime and (*b*) driven by the interior quasigeostrophic (QG) regime. The darkest and lightest regions represent extreme positive and negative values. Only one quarter of the computational domain is shown. Reprinted with permission from Scott (2006), copyright 2006, American Institute of Physics.

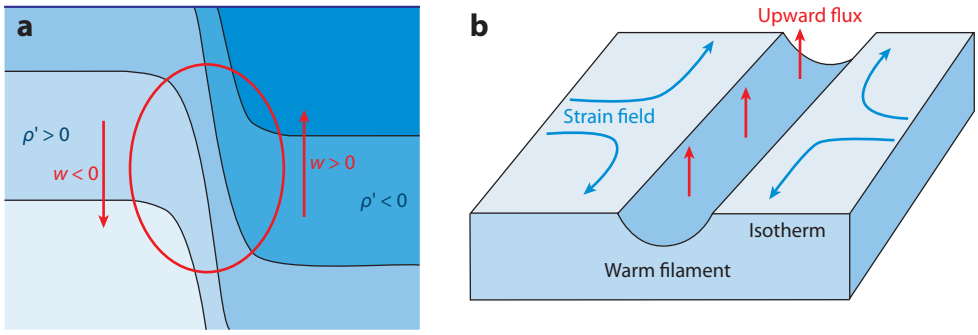

Figure 9

(*a*) Sketch of the ageostrophic circulation that develops in response to strengthening of a horizontal density front. The figure corresponds to a vertical cross section through a submesoscale front. Black lines are isopycnals. The red arrows correspond to the ageostrophic circulation. Lighter fluid (*dark blue*) is on the right of the figure and denser fluid (*light blue*) is on the left. (*b*) Schematic illustration of the vertical velocity field that develops in response to the elongation of a warm filament (*dark blue*) embedded in a horizontal strain field (*blue arrows*).

Such significant time evolution of the submesoscale structures, associated with large vorticity values, has a profound impact on the small-scale divergent field. The Omega equation (Equation 2) is still valid in this model and states that the vertical velocity is forced by a nonlinear term on the right-hand side that is proportional to the formation of small-scale density gradients (Hoskins 1982, Klein et al. 1998). Consequently, in response to this production of small-scale density fronts at the surface (not countered by the vertical velocity because $w = 0$ there), a vertical velocity field develops underneath (**Figure 9**). This differs from what happens in interior QG turbulence. Indeed three-dimensional motions in the interior are almost parallel to the isopycnals, which efficiently reduces the production of small-scale density fronts. Consequently, the submesoscale density gradients in the interior and their associated vertical velocities are weak (Klein et al. 1998). By contrast, in SQG, the small-scale vertical pump is strongly energized by the formation of small horizontal scales and the resulting surface frontogenesis processes. This phenomenon is the second major distinction from the interior QG regime. This difference is well illustrated by the analytical estimation given in **Figure 10**: The horizontal velocity is almost similar for the two regimes, but the vertical velocity is much larger in the SQG regime than in the interior QG regime for scales smaller than 100 km.

As a result, the root-mean-square (RMS) amplitude of the vertical velocity field is large, within either the eddy cores or the small-scale filaments outside the eddies (Lapeyre & Klein 2006b). The order of magnitude of this vertical pump is given by $w = Ro^2 B^{-1} H f_0$ (with $B = 1$ for these flows). However, the vertical pump is essentially at small scales and appears to be evenly partitioned between mesoscale eddies and small-scale elongated filaments between the eddies (Lapeyre & Klein 2006b). A final major result noted by Hakim and coworkers (2002) (another strong discrepancy with the interior QG regime) is that when the Rossby number is of order one, cyclonic structures dominate over anticyclonic structures, consistent with the in situ observations of Rudnick (2001).

What Is the Appropriate Regime for the Oceanic Flow?

The two divergent regimes described above involve a vertical pump with radically different properties. In the interior QG regime, the vertical velocity organizes mostly at the mesoscales and large values are found essentially within the eddies. In the SQG regime, larger values of vertical

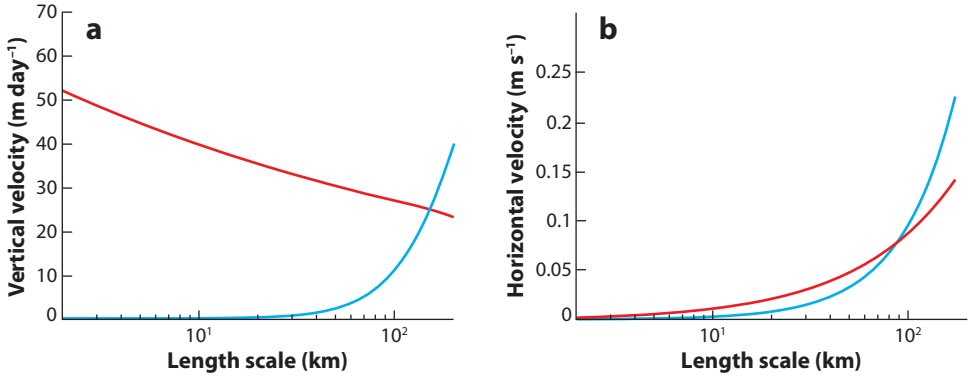

Figure 10

(*a*) Vertical velocity and (*b*) horizontal velocity at a 200-m depth as a function of the length scale for a quasigeostrophic (QG) interior baroclinic mode (*blue*) characterized by a k^{-3} velocity spectrum and a surface quasigeostrophic (SQG) mode (*red*) characterized by a $k^{-5/3}$ velocity spectrum. These velocities have been calculated assuming that the kinetic energy in both regimes is equal for the length scale of 100 km. The vertical velocity has been calculated using the Omega equation (Equation 2), assuming a large-scale strain field and constant stratification. SQG relations (Hakim et al. 2002) are used for the red curves. A cosine depth dependence is used for the stream function of the interior baroclinic mode, which allows one to get the density and then the vertical velocity (*blue curve in a*).

velocities can be found both within the submesoscale structures outside the eddies and around the eddies. This major difference is principally due to the impact of the surface frontogenesis (involving both mesoscales and small scales) present in the second regime. We may wonder whether in the real ocean only one particular regime is present or if a combination of both regimes exists. Recent theoretical analysis confirmed by high-resolution numerical simulations using primitive equation (PE) models provides some answers.

In the ocean, both dynamics are present because surface density anomalies and interior PV anomalies develop at the same time owing to the large-scale forcing in density. The question of the coupling of the boundary dynamics (driven by surface density) with the interior dynamics (driven by interior PV) was first addressed by Charney (1947) [see also Held (1978) and Pedlosky (1987)] in terms of baroclinic instability and eddy effects. Lapeyre & Klein (2006a), Scott (2006), and R. Tulloch & K.S. Smith (manuscript submitted) give further insight on the competition between SQG and interior QG dynamics. The order of magnitude of the maximum depth extension of the horizontal motions associated with the SQG mode is given by

$$h = \frac{f}{N}\frac{L_c}{2\pi}, \tag{5}$$

where L_c is the length scale that separates the interior QG mode (valid for larger scales) from the SQG mode (valid for smaller scales) and depends on the large-scale properties of the flow. For the upper ocean layers, $L_c = \mathrm{O}(100)$ km, which gives $h = 400$ m (using $N/f = 40$). This scale dependence was numerically confirmed in idealized configuration (Lapeyre & Klein 2006a; R. Tulloch & K.S. Smith, manuscript submitted). Smith (2007) and G. Lapeyre (manuscript submitted) have analyzed the pertinence of these ideas using realistic oceanic configurations at a basin scale. They show that the SQG mode dominates for horizontal scales up to 100–300 km in the Atlantic and Pacific.

Recent very-high-resolution simulations of mesoscale eddy turbulence (Capet et al. 2008a, Klein et al. 2008) that use PE models and a horizontal resolution up to 1/100° in the horizontal

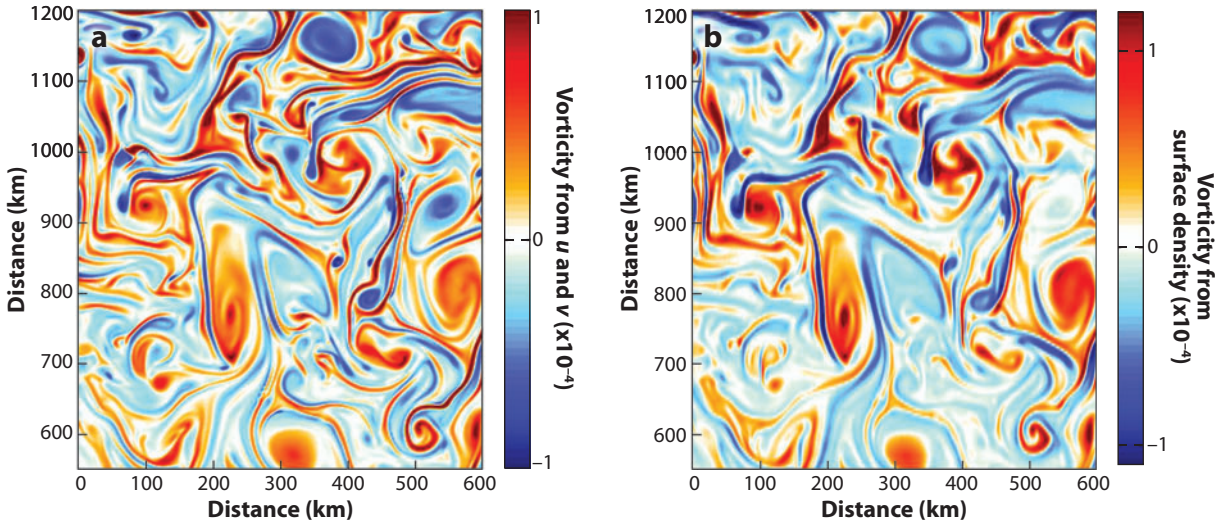

Figure 11

Snapshot of the surface relative vorticity field (*a*) deduced from u and v and (*b*) reconstructed from the surface density using surface quasigeostrophic (SQG) approximation. Vorticity units in s^{-1}. Adapted from Earth Simulator simulations described in Klein et al. (2008) with permission.

and 100 levels in the vertical nicely confirm the dominant contribution of the SQG mode in the surface layers for a range of scales up to 300 km. Results from Capet et al. (2008a,b) display a conspicuous k^{-2} spectrum slope for the kinetic energy in the surface layers, as expected for the SQG mode (Blumen 1978, Held et al. 1995), and highlight the role of the surface frontogenesis at small scale in this dynamics. Klein and coworkers (2008) have undertaken a more systematic comparison of their high-resolution PE solutions with the SQG dynamics: The velocity and density (when appropriately scaled) surface spectra are confounded and have a slope close to $k^{-5/3}$. Furthermore, well below the surface layers, QG dynamics is recovered as anticipated by Scott (2006). Finally, the vorticity field near the surface, reconstructed from the surface density using the SQG approximation, conspicuously matches the actual vorticity field (Klein et al. 2008) (**Figure 11**). Such a result is also confirmed by comparison of altimeter data (LeTraon et al. 2008) and SST from satellites that show that the SQG approximation is valid for the ocean surface (Isern-Fontanet et al. 2006a).

In terms of the vertical pump, the importance of the surface frontal scales was demonstrated by Nurser & Zhang (2000), Hakim and coworkers (2002), and Lapeyre and coworkers (2006). The divergent motions associated with the small-scale surface frontogenesis are large enough to trigger a significant restratification in the upper layers at a basin scale and in the absence of any cooling or heating (Hakim et al. 2002, Lapeyre et al. 2006). This restratification corresponds to a warming of the surface oceanic layers by almost one degree Celsius (over 100 days), compensated for by a cooling of the deeper layers. Also, results from Klein and coworkers (2008) show that increasing the spatial resolution by a factor of two leads to an increase by a factor of four of the vertical velocity RMS. This results from the dynamical impact of the small-scale surface density gradients. However, the depth extension of the resulting vertical velocity is usually much larger than h obtained by Equation 5 (Lévy et al. 2001, Klein et al. 2008), and therefore fully concerns (even for the vertical velocity associated with smaller-scale horizontal structures) the region well

below the mixed layer, where the tracer vertical gradients are large. Thus, this vertical pump driven by the submesoscale structures should significantly affect the vertical tracer fluxes at a global scale.

Some questions still remain. These questions concern a better estimation of the range of horizontal scales captured by the SQG dynamics (Smith 2007; G. Lapeyre, manuscript submitted). Another question pertains to the interaction between the SQG and interior regimes. This interaction should involve the vertical velocity field at small scale (Klein et al. 2008). A last question is about the dynamics associated with the smallest horizontal scales for which ageostrophic frontal instabilities must be better quantified (Molemaker et al. 2005; M. Molemaker, J. McWilliams & X. Capet, manuscript submitted).

CONCLUSION

The impact of the vertical exchanges of tracers due to mesoscale eddies has stimulated a large number of biogeochemical studies in the past decade. Important breakthroughs have been achieved. The quantification of these vertical exchanges (totally ignored in the past studies) indicates that they represent the second most important contribution to the annual nutrient requirement on a global scale. Further questions remain about what missed physical mechanisms could close the nutrient budget. Within this context, many studies such as those of Spall & Richards (2000) and Lévy and coworkers (2001) point out the impact of the submesoscales on the vertical exchanges as one of the most pertinent mechanisms. Still, very few assessments of this impact in a fully turbulent eddy field have been undertaken so far because of the lack of resolution in most studies. However, some results are stimulating. The rough estimations of Lapeyre & Klein (2006b), using a SQG model, quantify the potential impact of the submesoscale structures—versus mesoscale eddies—on the vertical nutrient fluxes on a global scale. Their estimates yield a contribution of 0.14 mol N m^{-2} $year^{-1}$ for the eddies and filaments in their close vicinity [which compares well with the total eddy contribution of McGillicuddy et al. (2003)] and 0.12 mol N m^{-2} $year^{-1}$ for the elongated filaments far off of the eddies. These submesoscale structures far off of the eddies allow the previous global geochemical estimates to almost double, which therefore could close the total nutrient budget. Treguer (2008) obtained the same results for the silicate in the Antarctic Circumpolar current. Furthermore, Lapeyre & Klein (2006b) showed that intermittent events, such as the encounter of an eddy with a stronger dipole, produce a very large number of small-scale filaments that trigger an intense vertical pump (**Figure 12**). Flierl & Davis (1993) and Anderson & Robinson (2001) reported that eddy-eddy or eddy-jet nonlinear interactions significantly increase the primary production in idealized simulations.

Conversely, recent fluid dynamical studies have revisited the turbulent mesoscale eddy regime and have demonstrated how the surface boundary condition may affect the turbulence properties through the submesoscales, driven by the surface frontogenesis. The issue of surface boundaries was considered by Charney (1971) and Blumen (1978), but did not receive enough attention at that time from a geophysical fluid dynamics (GFD) turbulence point of view. Because surface frontogenesis and associated ageostrophic processes are better resolved today by numerical simulations of mesoscale eddy turbulence, this subject has been revived, in particular for the upper ocean. The ongoing studies highlight that the vertical velocity field, or vertical pump, associated with the frontal submesoscales should principally affect the oceanic upper layers from the surface down to 500 m. One remaining question is how the surface and interior couple and how the vertical velocity field modifies this coupling.

Thus, there is a strong incentive from the ongoing studies, undertaken by both biogeochemists and dynamicists, to focus on the vertical pump driven by the submesoscale frontal structures near

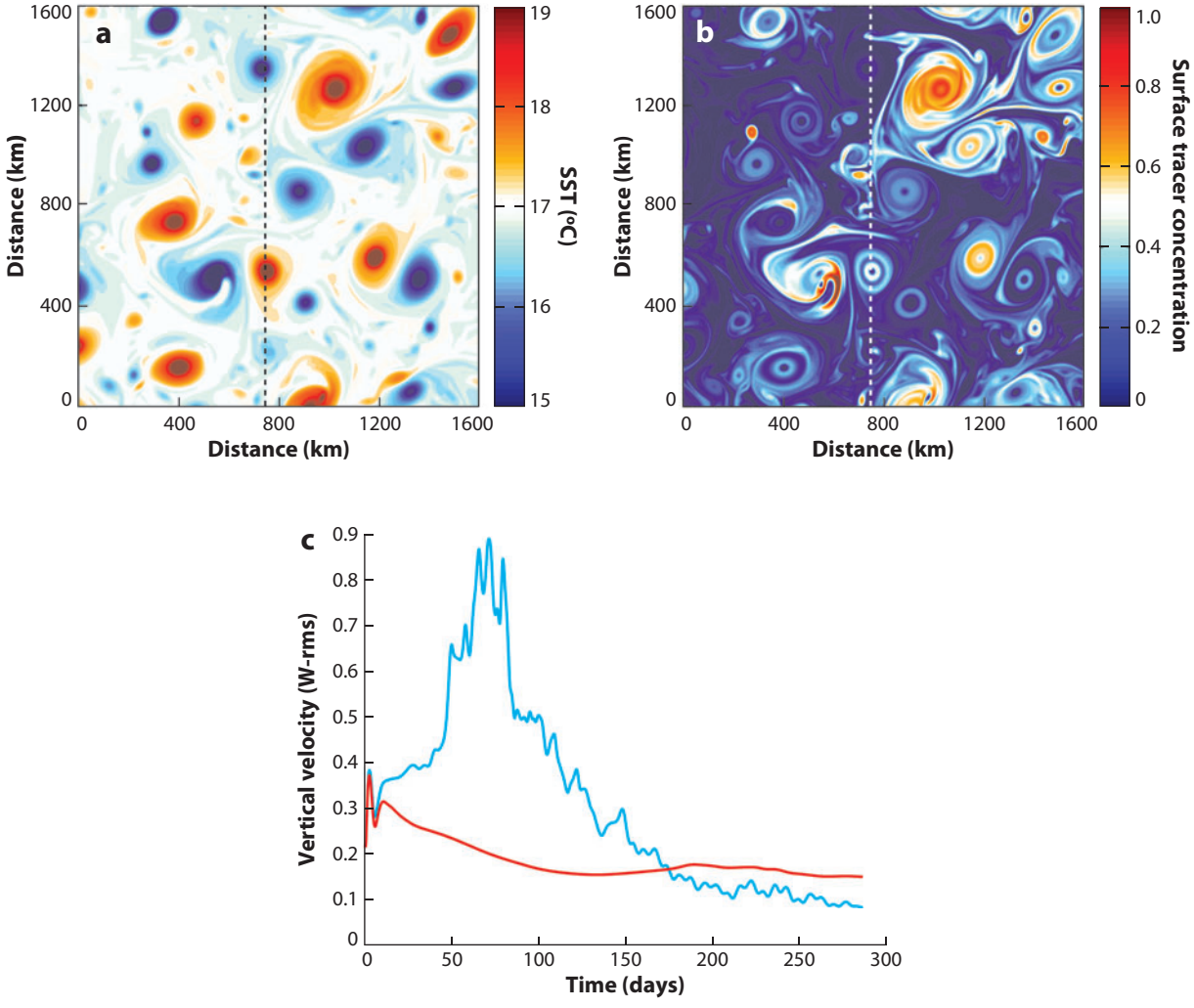

Figure 12

Horizontal snapshot of (*a*) sea surface temperature (SST) in degrees Celsius and (*b*) surface tracer concentration (nondimensional units). (*c*) *W*-rms evolution within a dipole alone (*red line*) and when the dipole encounters a third, much weaker eddy that subsequently merges (*blue line*). Such intermittent eddy merging leads to a strong increase of the vertical velocity that explains the high tracer concentration observed within eddies in the surface tracer field (*b*). Adapted from surface quasigeostrophic (SQG) simulations described in Lapeyre & Klein (2006b) with permission.

the ocean surface. This issue should be addressed in the coming decade with the expected strong increase of computer resources and the new and promising developments of in situ instruments such as Gliders. Indeed, adequate numerical simulations of ocean dynamics using PE models at a global scale with a spatial resolution of 3 km (and probably less) and at least 100 or 200 levels on the vertical should be affordable in the next five years. Addressing the impact of the small scales using ocean observations with the new expected instruments is another issue that would require in situ experiments designed to be driven principally by satellite observations in real time.

DISCLOSURE STATEMENT

The authors are not aware of any biases that might be perceived as affecting the objectivity of this review.

ACKNOWLEDGMENTS

The authors' work is supported by L'Institut Francais de Recherche pour l'Exploitation de la Mer (IFREMER) and Centre National de la Recherche Scientifique (CNRS) (France). P.K. also acknowledges the support from the French Agence Nationale pour la Recherche (Contract No. ANR-05-CIGC-010). We thank Bach Lien Hua, Guillaume Roullet, Paul Treguer, Marina Lévy, and Thierry Huck for useful comments.

LITERATURE CITED

Abraham ER. 1998. The generation of plankton patchiness by turbulent stirring. *Nature* 391:577–80

Abraham ER, Bowen MM. 2002. Chaotic stirring by a mesoscale surface-ocean flow. *Chaos* 12:373–81

Abraham ER, Law CS, Boyd PW, Lavender SJ, Maldonado MT, Bowle AR. 2000. Importance of stirring in the development of an iron-fertilized phytoplankton bloom. *Nature* 407:727–30

Allen CB, Kanda J, Laws EA. 1996. New production and photosynthetic rates within and outside a cyclonic mesoscale eddy in the north Pacific subtropical gyre. *Deep-Sea Res.* 43:917

Allen JT, Brown L, Sanders R, Moore CM, Mustard A, et al. 2005. Diatom carbon export enhanced by silicate upwelling in the northeast Atlantic. *Nature* 437:728–32

Allen JT, Smeed DA. 1996. Potential vorticity and vertical velocity at the Iceland-Færœs Front. *J. Phys. Oceanogr.* 26:2611–34

Allen JT, Smeeds D, Nurser J, Zhang J, Rixen M, Smeed A. 2001. Diagnosing vertical velocities using the QG omega equation: an examination of the errors due to sampling strategy. *Deep-Sea Res.* 26:2611–34

Anderson LA, Robinson AR. 2001. Physical and biological modeling in the gulf stream region. Part II. Physical and biological processes. *Deep-Sea Res.* I 48:1139–68

Blumen W. 1978. Uniform potential vorticity flow: Part I. Theory of wave interactions and two-dimensional turbulence. *J. Atmos. Sci.* 35:774–83

Bretherton FP. 1966. Critical layer instability in baroclinic flows. *Q. J. R. Meteorol. Soc.* 92:325–34

Capet X, Klein P, Hua B, Lapeyre G, McWilliams JC. 2008c. Surface kinetic energy transfer in surface quasi-geostrophic flows. *J. Fluid Mech.* 604:165–74

Capet X, McWilliams JC, Molemaker M, Shchepetkin A. 2008a. Mesoscale to submesoscale transition in the California current system. Part 1: Flow structure, eddy flux and observational tests. *J. Phys. Oceanogr.* 38:29–43

Capet X, McWilliams JC, Molemaker M, Shchepetkin A. 2008b. Mesoscale to submesoscale transition in the california current system. Part 2: Frontal processes. *J. Phys. Oceanogr.* 38:44–64

Charney J. 1971. Geostrophic turbulence. *J. Atmos. Sci.* 28:1087–95

Charney JG. 1947. The dynamics of long waves in a baroclinic westerly current. *J. Meteorol.* 4:135–62

Chelton DB, Schlax MG, Samelson RM, de Szoeke RA. 2007. Global observations of large oceanic eddies. *Geophys. Res. Lett.* 34:L15606. doi:10.1029/2007GL030812

Falkowski PG, Zieman D, Kolber Z, Bienfang PK. 1991. Role of eddy pumping in enhancing primary production in the ocean. *Nature* 352:55–58

Fasham MJR, Sarmiento JL, Slater RD, Ducklow HW, Williams R. 1993. Ecosystem behavior at bermuda station "S" and ocean weather station "India": a general circulation model and observational analysis. *Glob. Geochem. Cycles* 7:379–415

Flierl GR, Davis CS. 1993. Biological effects of gulf stream meandering. *J. Mar. Res.* 51:529–60

Fu L, Flierl G. 1980. Nonlinear energy and enstrophy transfers in a realistically stratified ocean. *Dyn. Atmos. Ocean.* 4:219–46

Garçon VC, Oschlies A, Doney SC, McGillicuddy D, Waniek J. 2001. The role of mesoscale variability on plankton dynamics in the north atlantic. *Deep-Sea Res.* II 48:2199–2226

Gill AE. 1984. On the behavior of internal waves in the wakes of storms. *J. Phys. Oceanogr.* 14:1129–51

Giordani LP, Caniaux G. 2005. Advanced insights into sources of vertical velocity in the ocean. *Ocean Dyn.* 56:513–24

Glover DM, Doney SC, Nelson NB, Wallis A, 2008. *Submesoscale anisotropy (fronts, eddies, and filaments) as observed near Bermuda with ocean color data*. Presented at Ocean Sci. Meet., Orlando.

Gower JFR, Denman KL, Holyer RJ. 1980. Phytoplankton patchiness indicates the fluctuation spectrum of mesoscale oceanic structure. *Nature* 288:157–59

Haine TW, Marshall J. 1998. Gravitational, symmetric, and baroclinic instability of the ocean mixed layer. *J. Phys. Oceanogr.* 28:634–58

Hakim GJ, Snyder C, Muraki DJ. 2002. A new surface model for cyclone-anticyclone asymmetry. *J. Atmos. Sci.* 59:2405–20

Held IM. 1978. The vertical scale of an unstable baroclinic wave and its importance for eddy heat flux parameterizations. *J. Atmos. Sci.* 35:572–76

Held IM, Larichev VD. 1996. A scaling theory for horizontally homogeneous, baroclinically unstable flow on a beta plane. *J. Atmos. Sci.* 53:946–52

Held IM, Pierrehumbert RT, Garner ST, Swanson KL. 1995. Surface quasi-geostrophic dynamics. *J. Fluid Mech.* 282:1–20

Hoskins BJ. 1982. The mathematical theory of frontogenesis. *Annu. Rev. Fluid Mech.* 14:131–51

Hoskins BJ, Draghici I, Davies HC. 1978. A new look at the ω-equation. *Q. J. R. Meteorol. Soc.* 104:31–38

Hua BL, Haidvogel DB. 1986. Numerical simulations of the vertical structure of quasi-geostrophic turbulence. *J. Atmos. Sci.* 43:2923–36

Hua BL, Klein P. 1998. An exact criterion for the stirring properties of nearly two-dimensional turbulence. *Physica D* 113:98–110

Hurlburt HE, Hogan PJ. 2000. Impact of 1/8° to 1/64° resolution on gulf stream model-data comparisons in basin-scale subtropical atlantic ocean models. *Dyn. Atmos. Ocean.* 32:283–329

Isern-Fontanet J, Chapron B, Lapeyre G, Klein P. 2006a. Potential use of microwave sea surface temperatures for the estimation of ocean currents. *Geophys. Res. Lett.* 33:L24608. doi: 10.1029/2006GL027801

Isern-Fontanet J, Garcia-Ladona E, Font J. 2006b. Vortices of the mediterranean sea: an altimetric perspective. *J. Phys. Oceanogr.* 36:87–103

Jenkins WJ. 1988. Nitrate flux into the euphotic zone near bermuda. *Nature* 331:521–23

Johannessen JA, Shuchman RA, Digranes G, Lyzenga DR, Wackerman C, et al. 1996. Coastal ocean fronts and eddies imaged with ERS 1 synthetic aperture radar. *J. Geophys. Res.* 101:6651–67

Juckes M. 1994. Quasigeostrophic dynamics of the tropopause. *J. Atmos. Sci.* 51:2756–68

Klein P, Hua BL, Lapeyre G. 2000. Alignment of tracer gradient vectors in 2D turbulence. *Physica D* 146:246–60

Klein P, Hua BL, Lapeyre G, Capet X, LeGentil S, Sasaki H. 2008. Upper ocean turbulence from high 3-D resolution simulations. *J. Phys. Oceanogr.* 38:1748–63

Klein P, Tréguier AM, Hua BL. 1998. Three-dimensional stirring of thermohaline fronts. *J. Mar. Res.* 56:589–612

LaCasce JH, Mahadevan A. 2006. Estimating subsurface horizontal and vertical velocities from sea surface temperature. *J. Mar. Res.* 64:695–721

Lapeyre G, Klein P. 2006a. Dynamics of the upper oceanic layers in terms of surface quasigeostrophy theory. *J. Phys. Oceanogr.* 36:165–76

Lapeyre G, Klein P. 2006b. Impact of the small-scale elongated filaments on the oceanic vertical pump. *J. Mar. Res.* 64:835–51

Lapeyre G, Klein P, Hua BL. 1999. Does the tracer gradient vector align with the strain eigenvectors in 2-D turbulence? *Phys. Fluids A* 11:3729–37

Lapeyre G, Klein P, Hua BL. 2006. Oceanic restratification by surface frontogenesis. *J. Phys. Oceanogr.* 36:1577–90

Larichev VD, McWilliams JC. 1991. Weakly decaying turbulence in an equivalent-barotropic fluid. *Phys. Fluids* 3:938–50

Ledwell JR, Watson AJ, Law CS. 1993. Evidence for slow mixing across the pycnocline from an open-ocean tracer-release experiment. *Nature* 364:701–703
Legal C, Klein P, Treguier AM, Paillet J. 2007. Diagnosis of the vertical motions in a mesoscale stirring region. *J. Phys. Oceanogr.* 37:1413–24
Lehahn Y, d'Ovidio F, Lévy M, Heitzel E. 2007. Stirring of the northeast atlantic spring bloom: a lagrangian analysis based on multi-satellite data. *J. Geophys. Res.* 112:C08005. doi:10.1029/2006JC003927
Le Traon PY, Klein P, Hua B, Dibarboure G. 2008. Do altimeter wavenumber spectra agree with the interior or surface quasi-geostrophic theory? *J. Phys. Oceanogr.* 38:1137–42
LeTraon PY, Morrow RM. 2001. Ocean current and eddies. In *Satellite Altimetry and Earth Sciences*, ed. LL Fu, A Cazenave, pp. 171–215. New York: Elsevier
Lévy M. 2008. The modulation of biological production by oceanic mesoscale turbulence. In *Transport in Geophysical Flow: Ten Years After*, ed. JB Weiss, A Provenzale, vol. 744 of *Lect. Notes Phys*. Berlin: Springer, pp. 219–61
Lévy M, Klein P. 2004. Does the low frequency of the mesoscale dynamics explain a part of the phytoplankton and zooplankton spectral variability? *Proc. R. Soc. London A* 460:1673–87
Lévy M, Klein P, Tréguier AM. 2001. Impact of submesoscale physics on production and subduction of phytoplankton in an oligotrophic regime. *J. Mar. Res.* 59:535–65
Lima ID, Olson DB, Doney SC. 2002. Biological response to frontal dynamics and mesoscale variability in oligotrophic environments: biological production and community structure. *J. Geophys. Res.* 107(C8):3111
López C, Neufeld Z, Hernández-García E, Haynes PH. 2001. Chaotic advection of reacting substances: plankton dynamics on a meandering jet. *Phys. Chem. Earth B* 26:313–17
Macvean MK, Woods JD. 1980. Redistribution of scalars during upper ocean frontogenesis: a numerical model. *Q. J. R. Meteorol. Soc.* 106:293–311
Mahadevan A, Archer D. 2000. Modeling the impact of fronts and mesoscale circulation on the nutrient supply and biochemistry of the upper ocean. *J. Geophys. Res.* 105:1209–25
Mahadevan A, Campbell J. 2002. Biogeochemical patchiness at the sea surface. *Geophys. Res. Lett.* 29(19):1926. doi:10.1029/2001GL014116
Mariotti A, Legras B, Dritschel DG. 1994. Vortex stripping and the erosion of coherent structures in two-dimensional flows. *Phys. Fluids A* 6:3954–62
Martin AP. 2003. Phytoplankton patchiness: the role of lateral stirring and mixing. *Prog. Oceanog.* 57:125–74
Martin AP, Pondaven P. 2003. On estimates for the vertical nitrate flux due to eddy pumping. *J. Geophys. Res.* 108(C11):3359. doi:10.1029/2003JC001841
Martin AP, Richards KJ. 2001. Mechanisms for vertical nutrient transport within a north atlantic mesoscale eddy. *Deep-Sea Res.* 48:757–73
Martin AP, Richards KJ, Bracco A, Provenzale A. 2002. Patchy productivity in the open ocean. *Glob. Geochem. Cycles* 16(2):1029
McGillicuddy DJ, Anderson L, Bates N, Bibby T, Buesseler KO, et al. 2007. Eddy/wind interactions stimulate extraordinary mid-ocean plankton blooms. *Science* 316:1021–26
McGillicuddy DJ, Anderson LA, Doney SC, Maltrud ME. 2003. Eddy-driven sources and sinks of nutrients in the upper ocean: result from a 0.1° resolution model of the north atlantic. *Glob. Geochem. Cycles* 17:1035
McGillicuddy DJ, Johnson R, Siegel DA, Michaels AF, Baters NR, Knap AH. 1999. Mesoscale variations of biogeochemical properties in the sargasso sea. *J. Geophys. Res.* 104:13381–94
McGillicuddy DJ, Kosnyrev VK, Ryan JP, Yoder JA. 2001. Covariation of mesoscale ocean color and sea surface temperature patterns in the sargasso sea. *Deep-Sea Res.* II 48:1823–36
McGillicuddy DJ, Robinson AR. 1997. Eddy-induced nutrient supply and new production in the sargasso sea. *Deep-Sea Res.* I 44:1427–50
McGillicuddy DJ, Robinson AR, Siegel DA, Jannasch HW, Johnson R, et al. 1998. Influence of mesoscale eddies on new production in the sargasso sea. *Nature* 394:263–66
McNeil JD, Jannasch HW, Dickey T, McGillicuddy D, Brzezinski MA, Sakamoto CM. 1999. New chemical, bio-optical, and physical observations of upper ocean response to the passage of a mesoscale eddy off bermuda. *J. Geophys. Res.* 104:15537–48
McWilliams JC. 1984. The emergence of isolated coherent vortices in turbulent flow. *J. Fluid Mech.* 146:21–43

McWilliams JC. 1989. Statistical properties of decaying geostrophic turbulence. *J. Fluid Mech.* 198:199–230
McWilliams JC. 1991. Geostrophic vortices. In *Nonlinear Topics in Ocean Physics, Proceedings of the International School of Physics, "Enrico Fermi" Course CIX*. ed. A.R. Osborne. Amsterdam: IOS Press
McWilliams JC. 2006. *Geophysical Fluid Dynamics: Fundamentals*. Cambridge, UK: Cambridge Univ. Press
Mizobata K, Saitoh SI, Shiomoto A, Miyamura T, Shiga N, et al. 2002. Bering sea cyclonic and anticyclonic eddies observed during summer 2000 and 2001. *Prog. Oceanogr.* 55:65–75
Molemaker M, McWilliams J, Yavneh I. 2005. Baroclinic instability and loss of balance. *J. Phys. Oceanogr.* 35:1505–17
Muraki DJ, Snyder C, Rotunno R. 1999. The next-order corrections to quasi-geostrophic theory. *J. Atmos. Sci.* 56:1547–60
Nurser AJG, Zhang JW. 2000. Eddy-induced mixed layer shallowing and mixed layer/thermocline exchange. *J. Geophys. Res.* 105:21851–68
Oschlies A. 2002a. Can eddies make ocean desert blooms? *Glob. Geochem. Cycles* 16:1830
Oschlies A. 2002b. Nutrient supply to the surface waters of the north atlantic: a model study. *J. Geophys. Res.* 107:275
Oschlies A, Garçon V. 1998. Eddy-induced enhancement of primary production in a model of the north atlantic ocean. *Nature* 394:266–69
Pedlosky J. 1987. *Geophysical Fluid Dynamics*. New York: Springer Verlag
Pierrehumbert RT, Held IM, Swanson KL. 1994. Spectra of local and nonlocal two-dimensional turbulence. *Chaos Solitons Fractals* 4:1111–16
Pollard RT, Regier LA. 1990. Large variations in potential vorticity at small spatial scales in the upper ocean. *Nature* 348:227–29
Pollard RT, Regier LA. 1992. Vorticity and vertical circulation at an ocean front. *J. Phys. Oceanogr.* 22:609–625
Polvani LM, McWilliams JC, Spall MA, Ford R. 1994. The coherent structures of shallow-water turbulence: deformation-radius effects, cyclone/anticyclone asymmetry and gravity-wave generation. *Chaos* 4:177–186
Rhines PB. 1979. Geostrophic turbulence. *Annu. Rev. Fluid Mech.* 11:404–441
Rhines PB. 1983. Lectures in geophysical fluid dynamics. *Lect. Appl. Math.* 20:3–58
Robinson A, McGillicuddy D, Calman J, Ducklow H, Fasham M, et al. 1993. Mesoscale and upper ocean variabilities during the 1989 JGOFS bloom study. *Deep-Sea Res.* 40:9–35
Rudnick DL. 1996. Intensive surveys of the azores front. 2. Inferring the geostrophic and vertical velocity fields. *J. Geophys. Res.* 101:16291–303
Rudnick DL. 2001. On the skewness of vorticity in the upper ocean. *Geophys. Res. Lett.* 28:2045–48
Salmon RS. 1980. Baroclinic instability and geostrophic turbulence. *Geophys. Astrophys. Fluid Dyn.* 15:167–211
Scott RK. 2006. Local and nonlocal advection of a passive scalar. *Phys. Fluids* 56:122–25
Shearman RK, Bath JA, Kosro PM. 1999. Diagnosis of the three-dimensional circulation associated with mesoscale motion in the california current. *J. Phys. Oceanogr.* 29:651–67
Siegel A, Weiss JB, Toomre J, McWilliams JC, Berloff PS, Yavneh I. 2001. Eddies and vortices in ocean basin dynamics. *Geophys. Res. Lett.* 28:3183–86
Siegel DA, McGillicuddy DJ, Fields EA. 1999. Mesoscale eddies, satellite altimetry, and new production in the sargasso sea. *J. Geophys. Res.* 104:13359–79
Smith KS. 2007. The geography of linear baroclinic instability in earth's oceans. *J. Mar. Res.* 29:655–83
Smith KS, Vallis GK. 2001. The scales and equilibration of midocean eddies: freely evolving flow. *J. Phys. Oceanogr.* 31:554–71
Smith KS, Vallis GK. 2002. The scales and equilibration of midocean eddies: forced-dissipative flows. *J. Phys. Oceanogr.* 32:1699–721
Spall MA. 1995. Frontogenesis, subduction, and cross-front exchange at upper ocean fronts. *J. Geophys. Res.* 100:2543–57
Spall SA, Richards KJ. 2000. A numerical model of mesoscale frontal instabilities and plankton dynamics: I. Model formulation and initial experiments. *Deep-Sea Res.* 47:1261–301
Stapleton NR, Aicken WT, Dovey PR, Scott JC. 2002. The use of radar altimeter data in combination with other satellite sensors for routine monitoring of the ocean: case study of the northern Arabian Sea and Gulf of Oman. *Can. J. Remote Sens.* 28:567–72

Strass VH. 1992. Chlorophyll patchiness caused by mesoscale upwelling at fronts. *Deep-Sea Res.* 39:75–96
Tintoré J, Gomis D, Alonso S, Parrilla G. 1991. Mesoscale dynamics and vertical motion in the alboran sea. *J. Phys. Oceanogr.* 21:811–23
Treguer PJ, 2008. *New perspectives in the Si marine biogeochemistry*. Presented at Ocean Sci. Meet., Orlando.
Tulloch R, Smith KS. 2006. A new theory for the atmospheric energy spectrum: Depth-limited temperature anomalies at the tropopause. *Proc. Nat. Am. Soc.* 103:14690–94
Vallis GK. 2006. *Atmospheric and Oceanic Fluid Dynamics*. Cambridge, UK: Cambridge Univ. Press
Viudez A, Dritschel DG. 2004. Dynamic potential vorticity initialization and the diagnosis of mesoscale motion. *J. Phys. Oceanogr.* 34:2761–73
Waugh DW, Dritschel DG. 1991. The stability of filamentary in two-dimensional geophysical vortex-dynamics models. *J. Fluid Mech.* 231:575–98
Weiss J. 1991. The dynamics of enstrophy transfer in two-dimensional hydrodynamics. *Physica D* 48:273–94
Welander P. 1955. Studies on the general development of motion in a two dimensional ideal fluid. *Tellus* 7:141–56

Annual Review of
Marine Science

Volume 1, 2009

Contents

Errata

An online log of corrections to *Annual Review of Marine Science* articles may be found at http://marine.annualreviews.org/errata.shtml